A Hybrid UHF RFID Tag Robust to Host Material

Abed Pour Sohrab, *Student Member, IEEE*, Yi Huang, *Senior member, IEEE*, Muaad Hussein, *Student Member, IEEE*, Manoj Stanley, *Student Member, IEEE*, and Paul Carter

***Abstract*—A novel hybrid UHF RFID tag is proposed in this paper. Most of the available UHF RFID tags are either label-type dipole or patch antennas which are designed for non-metallic and metallic objects, respectively. The label-type dipoles are not functional on metallic objects and patch antennas are not efficient on non-metallic objects in terms of read range and radiation pattern. The proposed hybrid tag offers the advantage of both dipole type and patch antenna depending on the object it is placed on. This dual port tag is capable of working in two different modes in off-metal and on-metal scenarios. In off-metal mode, the tag works as a dipole antenna designed on an FR-4 substrate with 3.2 mm thickness. The wide capacitive loaded dipole arms and optimum tuned impedance matching between the chip and the antenna increase the robustness in off-metal mode. The role of critical parts of the tag in impedance matching is investigated on Smith chart. The result of this study suggests a straightforward technic for fine tuning of any type of dipole tag. The metallic surface of the host material acts as the ground plane in on-metal mode and the tag transforms into a short-ended quarter wavelength patch antenna. The resonant frequency in this mode can be tuned using the slots designed at the edge of the patch. The measurement result confirms an outstanding read range on different materials.**

***Index Terms*— Equivalent circuits, impedance matching, radio frequency identification (RFID), RFID tag antennas, Smith chart.**

I. Introduction

PASSIVE radio frequency identification (RFID) tags working in ultra-high frequency (UHF) band (840-960 MHz) offer an outstanding read range and high rate of data capacity stored in the RFID chip. The development of this technology in recent years has been not only introduced as a principal solution for object tracking applications but also made it a key component in different applications like parking management systems, wireless sensors, and indoor navigation systems [1], [2].

According to the diversity of the application, the RFID tags need to be attached on different objects which include materials with high dielectric constant and also metallic objects. UHF RFID tags can be categorized into two different groups: label-type and substrate based tags. Label-type tags are usually used for tagging non-metallic objects [3]-[6]. A common problem of this type of tags is detuning effect and it happens when the dielectric properties of the host material affects the frequency response of the tag antenna [7]. Reducing the quality factor and increasing the bandwidth is a practiced solution to improve the robustness of the tag. This can be done either by having thicker elements in the body of the tag or adding capacitive loads to the tip of the dipole tag [7]-[9]. The label-type dipole tags are not suitable for tagging metallic objects [10]. Substrate based antennas employing a ground plane are usually used for this purpose. The ground plane and metallic surface of the host material increases the directivity and gain of the antenna [8]. Different types of patch antenna are proposed in literature. In some designs the patch is connected to the ground by folding the edge or using vias [11]-[14]. Connection to the ground plane is eliminated by using a slot patch in [15] or applying a decoupling intermediate layer between the patch and ground plane in [16]. Planar inverted-F antenna (PIFA) tag design is another solution for metallic objects [17]. Tag designs are supported by artificial ground plane made by periodic structures in [18], [19]. Cavity backed patch tag design is proposed in [20]. In some designs there is no ground plane and the body of the metallic object acts as a ground plane when the tag is placed on it. The design might be able to work on non-metallic objects but the performance is limited compared to conventional label-type tags [21], [22]. More work was reviewed in [2].

The stability in performance and optimum reading range on different materials are two important factors in tagging objects. The challenge is to have a single design which can fulfill these requirements. The label-type dipole tag offers a desirable omnidirectional radiation pattern perpendicular to the dipole axis but it is not functional on metallic bodies. On the other hand the tags with a ground plane offer outstanding read range on metallic bodies but lower read range on non-metallic objects. In addition, directive radiation pattern is not desirable for tagging non-metallic materials. Therefore, none of the reviewed tags are efficient on all materials.

The target of this study is to suggest a tag design that shows the advantages of both mentioned groups: Omnidirectional radiation pattern on non-metallic objects and improved directive gain on metallic host materials with acceptable read

This work is supported by Aeternum, LLC.

A. P. Sohrab, Y. Huang, M. Hussein, and M. Stanley are with the Department of Electrical Engineering and Electronics, University of Liverpool, Brownlow Hill, Liverpool L69 3GJ, United Kingdom (e-mail: yi.huang@liv.ac.uk).

P. Carter is with Aeternum, LLC., 23475 Rock Haven Way, # 165, Dulles, VA, USA.

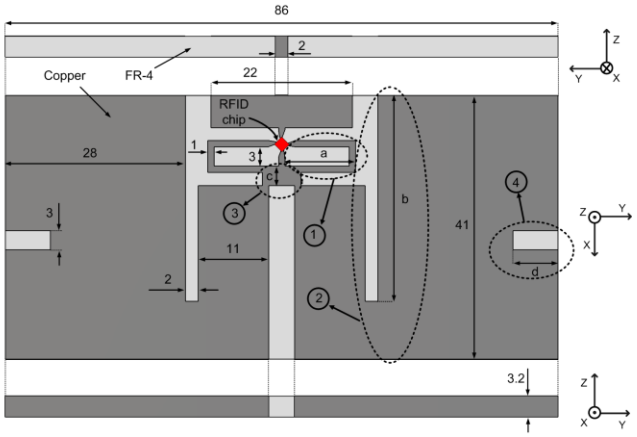

Fig. 1. Structure of the proposed design. a = 11.5, b = 32, c = 2, and d=9. All the values are in millimeters.

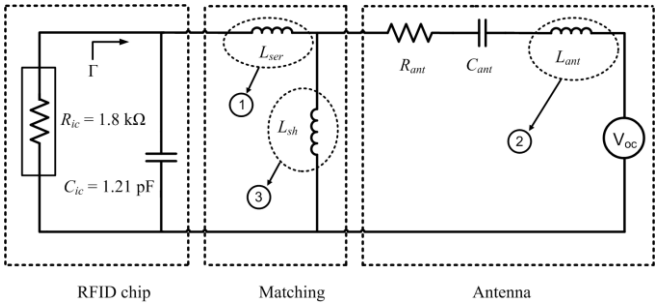

Fig. 2. Equivalent circuit of the proposed tag design working in off-metal mode.

range in both cases. A novel hybrid UHF RFID tag is proposed in this paper which works in two different modes. In one mode the tag works as a dipole antenna on non-metallic objects and in the other mode it works as a short ended quarter wavelength patch antenna on metallic objects. The design analysis in two different modes is presented in next section followed by the fabrication and measurement results.

II. Tag Design Analysis

The structure of the proposed design is depicted in Fig. 1. A Monza 4 Dura RFID chip is used in the design. This chip has a dual port input which is basically provided for dual polarized symmetric tag designs for having a uniform radiation pattern [23]. However the chip can be used for other purposes as the two ports are working independently. For example, a dual band design is proposed using this chip in [24]. In conventional antenna designs, the antenna port is usually matched to 50 Ω; but in passive RFID tag designs, the antenna needs to be conjugate matched to the complex input impedance of the RFID chip [3]. According to internal capacitive components for saving power, RFID chips have capacitive input impedance which demands antenna design with inductive input impedance. The complex input impedance of Monza 4 is Z_{chip} = 13-j151 at 866 MHz. Thus the input impedance of the antenna should be Z_{ant} = 13+j151 for perfect matching. As mentioned earlier, the tag works in two different modes. Each port of the chip is activated in one mode. We analyze these two modes in the following

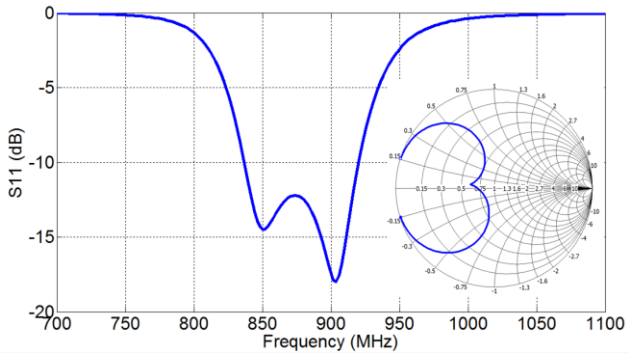

Fig. 3. Optimum frequency response of the tag in off-metal mode. The Smith chart is normalized to 1.8 kΩ.

subsections.

A. Off-metal Mode

The horizontal port of the chip is activated in this mode. This port is in the direction of Y axis shown in Fig. 1. The antenna is comprised of a dipole which is matched to the chip using an inductive loop [5]. The equivalent circuit of the tag in off-metal mode is also shown in Fig. 2. This circuit is used for most dipole based tag designs [8]. Perfect impedance matching between the chip and antenna is necessary for achieving the maximum reading range [2]. Although it is feasible to analyze the equivalent circuit using simulation software and translate the different parts of the physical structure to the circuit elements using approximate equations but a fine tuning of the dimensions is required at the end to have a perfect impedance matching [25]. In this section, we analyze different parts of the antenna and its effect on the impedance matching. The result of this study can be generalized as a straightforward technic for fine tuning of any type of dipole based UHF RFID tag. The input impedance of Monza 4 is equivalent to 1.8 kΩ resistance in parallel to 1.21 pF capacitance as depicted in Fig. 2. The position of the desired input impedance of the tag antenna for having a conjugate match (Z_{ant} = 13+j151) would be close to the rim of the Smith chart normalized to 50 Ω [13], [17]. Studying the impedance matching is not easy at this point. It is better to normalize the Smith chart to Z_{ant} for having the match point at the center of the chart. Some simulation tools are not capable of normalizing the Smith chart to a complex load. The suggested solution by authors is to assume the capacitance of the chip as part of the antenna and consider the matching between the 1.8 kΩ resistor and the rest of the circuit as illustrated in Fig. 2. The Smith chart should be normalized to 1.8 kΩ in this method. The frequency response of the tuned design is shown in Fig. 3. The notch on the plot close to the center of Smith chart represents the existence of two resonances which are created by the series RLC combination in dipole arm and the parallel RLC combination of the chip and inductive matching loop [25].

The tag structure of Fig. 1 is divided into different critical parts distinguished by numbers and the corresponding elements in the equivalent circuit are illustrated in Fig. 2. We analyze the effect of altering each part of the design on

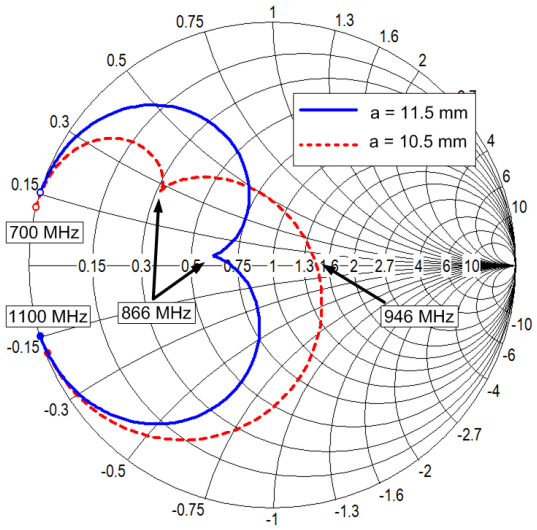

Fig. 4. Reducing the length of part (1) in Fig. 1 and its effect on the frequency response in Smith chart.

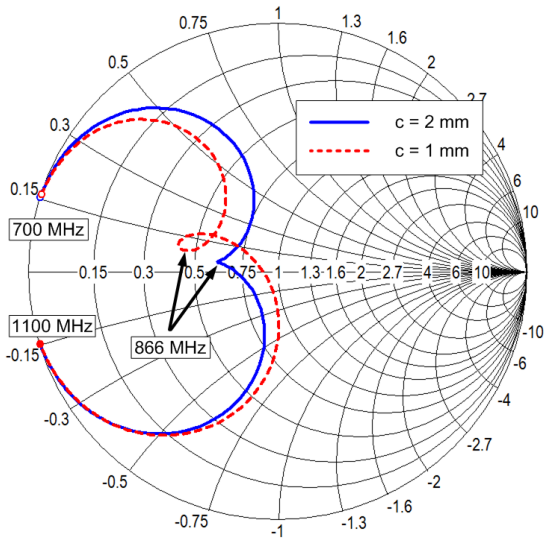

Fig. 6. Reducing the width of part (3) in Fig. 1 and its effect on the frequency response in Smith chart.

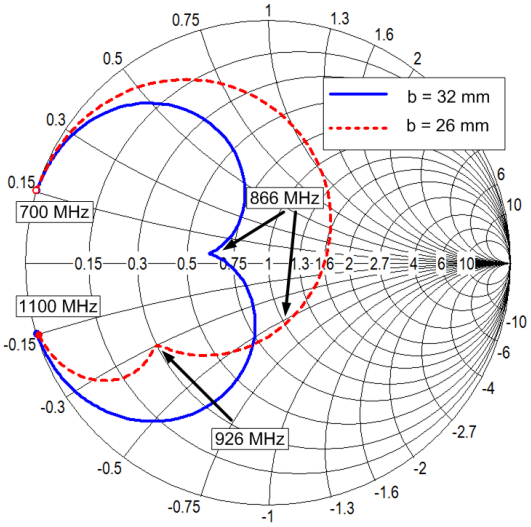

Fig. 5. Reducing the length of part (2) in Fig. 1 and its effect on the frequency response in Smith chart.

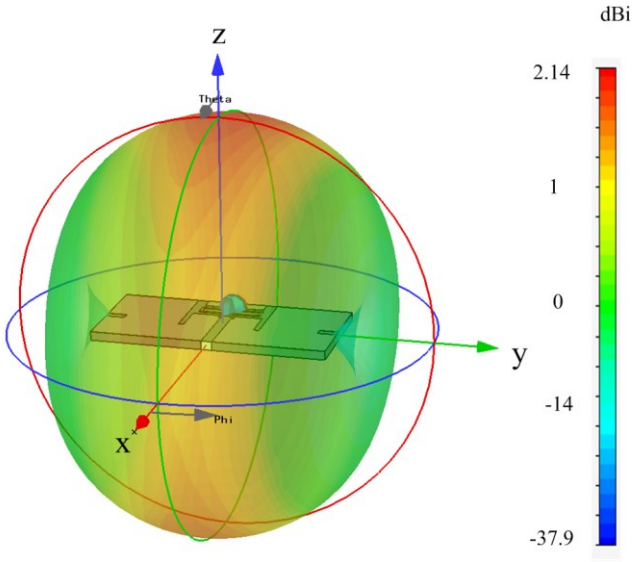

Fig. 7. Radiation pattern of the tag in free space working in off-metal mode.

impedance matching. The effect of reducing the length of the matching loop in part one, which is equivalent to reducing the inductance L_{ser}, is investigated in Fig. 4. As can be seen, the total plot moves in a counter-clockwise direction which shifts the higher frequencies to the center of the chart.

Reducing the length of the slot in the second part of the antenna is mainly equivalent to reducing the inductance L_{ant} in the circuit. The consequence of this change is moving the notch on the plot towards higher frequencies in a clockwise direction as shown in Fig. 5. The effect of reducing the capacitance C_{ant}, which is equal to reducing the area of the dipole, is almost similar to the plot of Fig. 5.

The third part of the antenna is equivalent to inductance L_{sh}. Reducing the thickness of this part causes an increase in the value of inductance. This transforms the notch on the plot to a loop as depicted in Fig. 6. The diameter of this loop can be further increased by increasing the value of inductance. The bandwidth of the frequency response can be controlled by this part. According to the application and working frequency of the tag, the optimum frequency response is not always achieved by having a plot passing through the center of the Smith chart but the detuning effect of the background materials should also be considered as well. The radiation resistance R_{ant} is mainly affected by the length of the dipole [8]. The effect of increasing the value of this element is almost similar to the plot of Fig. 6 which can be another way for controlling the bandwidth.

One of the advantages of the proposed tag is that there is no ground plane in the back of the substrate in off-metal mode. Thus, the radiation pattern is uniform around the axis of the dipole as shown in Fig. 7. This makes the tag readable from different angles.

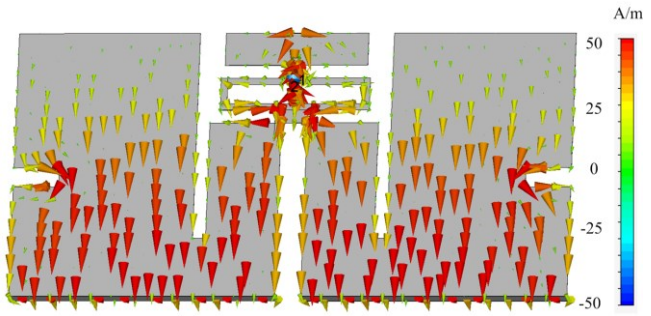

Fig. 8. Surface currents of the design working in on-metal mode.

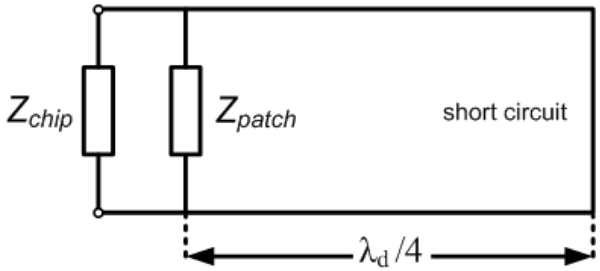

Fig. 9. Equivalent circuit model of the tag working in on-metal mode.

B. On-metal Mode

The vertical port of Monza 4 is activated in on-metal mode. This port is in the direction of X axis as shown in Fig. 1. The metallic surface of the host material acts as the ground plane and the tag transforms from a dipole to a patch antenna. The relative dielectric constant of the FR-4 substrate is around 4.3. This increases the electrical length of the patch antenna. According to the following equation:

$$\lambda_d = \frac{\lambda_0}{\sqrt{\varepsilon_r}} \tag{1}$$

the wavelength in the X axis direction of the patch (λ_d) is shorter than the wavelength in free space (λ_0). The length of the patch antenna shown in Fig. 1 is 41 mm which is roughly equal to quarter wavelength at 866 MHz. The patch antenna is shorted to the ground using the conductive walls located at the lower edge of the design shown in the bottom of Fig. 1. This short circuit is seen as an open circuit from the location of the chip as the patch behaves like a quarter wavelength transformer. The surface currents on the patch start from a low level at the location of the chip and reach a maximum after passing the quarter wavelength path as shown in Fig. 8. The high currents guarantee acceptable radiation efficiency despite the small thickness of the tag. The currents at the location of the chip are lower and the voltage between the patch and the ground is higher. This condition provides appropriate input impedance for matching with the chip [8]. One side of the chip port is connected to the patch whereas the other side needs to be connected to the ground. This is done using the metallic strip located at the upper edge of the design depicted in the top of Fig. 1. The excited electric field at this edge is the source of radiation in this antenna.

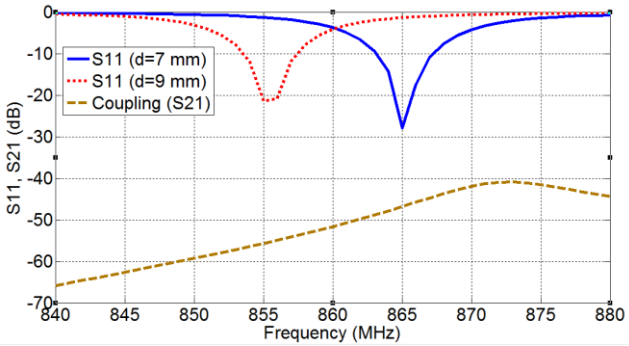

Fig. 10. Frequency response of the tuned tag working in on-metal mode and the effect of increasing the length of the slot in part (4) of Fig. 1; Coupling between two ports of the chip.

The equivalent circuit of the tag working in on-metal mode is shown in Fig. 9. Similar to the off-metal mode, a conjugate impedance matching to the chip is required here. The input impedance of the patch is mainly dependent on the position of the chip port along X axis, the width of the patch along Y axis, and the slot in part (2) of the design shown in Fig. 1. However, all these parameters also affect the matching in off-metal mode. A practical approach for the designer is to tune the tag simultaneously at both modes using the analysis results.

The tuned frequency response of the tag is illustrated in Fig. 10. Although the bandwidth of the tag in this mode is less than the off-metal mode but it is sufficient for running the chip at 866 MHz. The mutual coupling between the two ports is an undesirable factor that should be kept as low as possible. High degree of coupling causes a loss in the induced power which affects the performance. Symmetry of the design in Y axis direction helps to limit the coupling effect. The surface currents shown in Fig. 8 are in symmetry according to the horizontal port of the chip. This induces the same voltage at both sides of the horizontal port and reduces the coupling effect consequently. The level of coupling between two ports is also plotted in Fig 10. The slot located at part (4) of the design in Fig. 1 can be used for fine tuning of the tag in on-metal mode. The frequency response of the tag can be shifted by changing the length of this slot as shown in Fig. 10. Increasing the length of this slot makes the surface currents to pass through a longer path which reduces the resonant frequency. This change does not have a significant effect on the frequency response of the tag in off-metal mode because the slot is located at the tip of the dipole where the currents are small at that mode.

The gain of the tag is dependent on the size of the metallic host material. The directivity of the design can reach up to 6.19 dBi by placing it on a 20 cm × 20 cm metallic plate as shown in Fig. 11.

III. Fabrication and Measurement Results

The proposed design of Fig. 1 is etched on an FR-4 substrate and Monza 4 Dura is soldered to the two input ports of the tag as shown in Fig. 12. The theoretical read range of

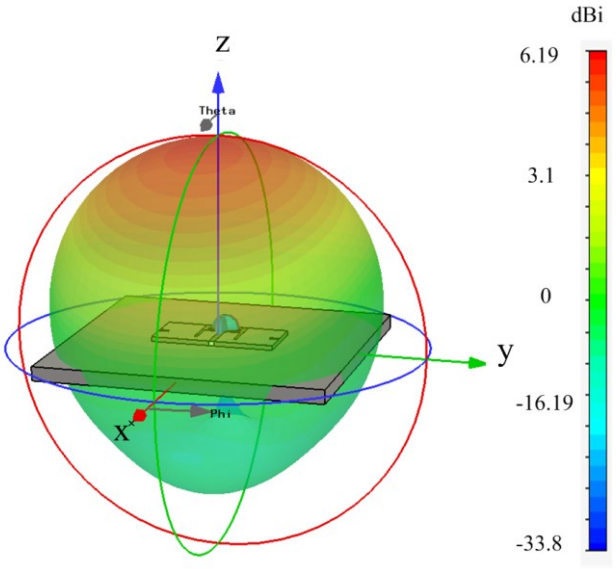

Fig. 11. Radiation pattern of the tag on a 20 cm × 20 cm metallic plate.

Fig. 12. Prototype of the proposed design and measurement setup in anechoic chamber.

the tag can be predicted using Friis formula:

$$d_{tag} = \frac{\lambda}{4\pi}\sqrt{\frac{\chi \tau e_{r,tag} D_{tag} EIRP}{P_{ic}}} \quad (2)$$

where, λ is the wavelength of the carrier tone; χ is the mutual polarization power efficiency between the tag and reader antenna; τ is the antenna-chip power transfer efficiency; $e_{r,tag}$ is the radiation efficiency of the tag antenna; D_{tag} is the tag antenna directivity; *EIRP* is the equivalent isotropic radiated power of the reader; and P_{ic} is the wakeup power of the tag chip [2]. However, the calculated reading range using this formula is not always accurate due to different errors in design simulation, fabrication and testing process. A practical approach for finding the maximum read range with maximum regulated *EIRP* is to measure the read range with a smaller *EIRP* first and find the maximum read range using:

$$d_{\max} = d_{ref}\sqrt{\frac{EIRP_{\max}}{EIRP_{ref}}} \quad (3)$$

TABLE I
READING RANGE OF THE TAG IN CENTIMETERS

Material	EIRP=0.63 W	EIRP=4 W
Free space	270	680
Aluminum plate	150	378
Wood	192	484
Ceramic	155	391
Glass	115	290

where d_{max} is the maximum possible tag read range, d_{ref} is the reference read range measured in the lab, $EIRP_{max}$ represents the maximum regulated *EIRP* which is 4 Watts in most regions, and $EIRP_{ref}$ is for the equipment used to measure the reference read range in the lab. For example, a Nordic ID PL3000 UHF RFID reader which is a handheld device with 630 mW *EIRP* is used in our tests in an anechoic chamber as illustrated in Fig. 12. The reference measured read range of the tag placed on a 20 cm × 20 cm aluminum plate is 111 cm. Thus, the maximum read range would be 280 cm using (3).

The performance of the tag in off-metal mode is also measured using the same method and equipment on a different range of materials. The results are tabulated in Table I. The tag shows robustness to challenging materials. This means a limited detuning effect and can be referred to following reasons:

- The frequency response of the tag is optimally tuned and there is a perfect impedance matching between the chip and antenna.
- The FR-4 substrate prevents the dipole from close contact to the host material and limits its effect on the dipole characteristics.
- The capacitive loaded wide dipole arms increase the bandwidth and robustness of the tag to high dielectric materials.

As mentioned earlier, the metallic surface of host material works as the ground plane in on-metal performance. Thus, for metalic materials with non-flat surface the read range might be degraded. In this case, a metallic sticker foil can be attached to the back of the design as a ground plane.

IV. CONCLUSION

It was shown in this paper that the proposed hybrid UHF RFID tag uniquely offers the omnidirectional radiation pattern of a dipole on non-metallic objects and directive pattern of a patch antenna on metallic objects which makes it capable of working efficiently on a wide range of materials. Single port designs which can run the conventional RFID chips might be considered as extension of the proposed design in future.

REFERENCES

[1] K. Finkenzeller, "Introduction," in *RFID handbook: fundamentals and applications in contactless smart cards and identification*' 2nd ed. New York: John Wiley & Sons, 2003, pp. 1-7.

[2] T. Bjorninen, L. Sydanheimo, L. Ukkonen, Y. Rahmat-Samii, "Advances in antenna designs for UHF RFID tags mountable on conductive items," *IEEE Antennas Propag. Magaz*., vol. 56, no. 1, pp. 79-103, 2014.
[3] K. V. S. Rao, P. V. Nikitin, and S. F. Lam, "Antenna design for UHF RFID tags: A review and a practical application," *IEEE Trans. Antennas Propag.*, vol. 53, pp. 3870–3876, Dec. 2005.
[4] G. Marrocco, "The art of UHF RFID antenna design: impedance-matching and size-reduction techniques," *IEEE Antennas Propag. Magaz.*, vol. 50, no. 1, pp. 66-79, Feb. 2008.
[5] G. Zamora, S. Zuffanelli, F. Paredes, F. Martin, and J. Bonache, "Design and Synthesis Methodology for UHF-RFID Tags Based on the T-Match Network," *IEEE Trans. Microw. Theory Tech.*, vol. 61, no. 12, pp. 4090-4098, Dec. 2013.
[6] S. Zuffanelli, G. Zamora, P. Aguilà, F. Paredes, F. Martín and J. Bonache, "Analysis of the Split Ring Resonator (SRR) Antenna Applied to Passive UHF-RFID Tag Design," *IEEE Trans. Antennas Propag.*, vol. 64, no. 3, pp. 856-864, March 2016.
[7] Shuai Shao, R. J. Burkholder and J. L. Volakis, "Design Approach for Robust UHF RFID Tag Antennas Mounted on a Plurality of Dielectric Surfaces," *IEEE Antennas Propag. Magaz.*, vol. 56, no. 5, pp. 158-166, Oct. 2014.
[8] D. M. Dobkin, "Tag Antennas," in *The RF in RFID: Passive UHF RFID in Practice*, Newnes, 2007.
[9] A. P. Sohrab, Y. Huang, M. Kod, M. Hussein and P. Carter, "Label-type 3D RFID tag mountable on metallic and non-metallic objects," in *Loughborough Anennas. & Propag. Conf. (LAPC)*, Loughborough, United Kingdom, 2016, pp. 1-3.
[10] D. M. Dobkin and S. M. Weigand, "Environmental effects on RFID tag antennas," in *Microwave Symp. Digest, 2005 IEEE MTT-S Internationl*, June 12-17, 2005, pp. 4.
[11] A. G. Santiago, J. R. Costa and C. A. Fernandes, "Broadband UHF RFID Passive Tag Antenna for Near-Body Applications," *IEEE Antennas Wireless Propag. Lett.*, vol. 12, pp. 136-139, 2013.
[12] K. H. Lin, S. L. Chen and R. Mittra, "A Looped-Bowtie RFID Tag Antenna Design for Metallic Objects," in *IEEE Trans. Antennas Propag.*, vol. 61, no. 2, pp. 499-505, Feb. 2013.
[13] M. Polivka, M. Svanda, "Stepped impedance coupled-patches tag antenna for platform-tolerant UHF RFID applications," *IEEE Trans. Antennas Propag.*, vol. 63, no. 9, pp. 3791-3797, 2015.
[14] F. L. Bong, E. H. Lim and F. L. Lo, "Flexible Folded-Patch Antenna With Serrated Edges for Metal-Mountable UHF RFID Tag," *IEEE Trans. Antennas Propag.*, vol. 65, no. 2, pp. 873-877, Feb. 2017.
[15] A. Dubok and A. B. Smolders, "Miniaturization of Robust UHF RFID Antennas for Use on Perishable Goods and Human Bodies," *IEEE Antennas Wireless Propag. Lette.*, vol. 13, pp. 1321-1324, 2014.
[16] J. Choo and J. Ryoo, "UHF RFID Tag Applicable to Various Objects," *IEEE Trans. Antennas and Propag.*, vol. 62, no. 2, pp. 922-925, Feb. 2014.
[17] M. Hirvonen, K. Jaakkola, P. Pursula and J. Saily, "Dual-Band Platform Tolerant Antennas for Radio-Frequency Identification," *IEEE Trans. Antennas Propag.*, vol. 54, no. 9, pp. 2632-2637, Sept. 2006.
[18] D. Kim and J. Yeo, "Dual-Band Long-Range Passive RFID Tag Antenna Using an AMC Ground Plane," *IEEE Trans. Antennas Propag.*, vol. 60, no. 6, pp. 2620-2626, June 2012.
[19] B. Gao and M. M. F. Yuen, "Passive UHF RFID Packaging With Electromagnetic Band Gap (EBG) Material for Metallic Objects Tracking," *IEEE Trans. Components Packag. Manufac. Tech.*, vol. 1, no. 8, pp. 1140-1146, Aug. 2011.
[20] H. Sun, B. Tao and O. M. Ramahi, "Proximity Coupled Cavity Backed Patch Antenna for Long Range UHF RFID Tag," *IEEE Trans. Antennas Propag.*, vol. 64, no. 12, pp. 5446-5449, Dec. 2016.
[21] J. Dacuna and R. Pous, "Low-Profile Patch Antenna for RF Identification Applications," *IEEE Trans. Microw. Theory Tech.*, vol. 57, no. 5, pp. 1406-1410, May 2009.
[22] T. W. Koo, D. Kim, J. I. Ryu, H. M. Seo, J. G. Yook and J. C. Kim, "Design of a Label-Typed UHF RFID Tag Antenna for Metallic Objects," *IEEE Antennas Wireless Propag. Lett.*, vol. 10, pp. 1010-1014, 2011.
[23] Monza 4 tag chip datasheet (2016). [Online]. Available: https://support.impinj.com/hc/en-us/articles/202756908-Monza-4-RFID-Tag-Chip-Datasheet
[24] G. H. Du, T. Tang and Y. Deng, "Dual-band metal skin UHF RFID tag antenna," *Electronics Letters*, vol. 49, no. 14, pp. 858-860, July 4 2013.
[25] A. P. Sohrab, Y. Huang, M. Hussein, M. Kod and P. Carter, "A UHF RFID Tag With Improved Performance on Liquid Bottles," *IEEE Antennas Wireless Propag. Lett.*, vol. 15, pp. 1673-1676, 2016.